ACS APPLIED MATERIALS & INTERFACES

Letter

www.acsami.org

Electrospray Formation of Gelled Nano-Aluminum Microspheres with Superior Reactivity

Haiyang Wang,[†] Guoqiang Jian, Shi Yan,[†] Jeffery B. DeLisio, Chuan Huang,[†] and Michael R. Zachariah*

Department of Chemical and Biomolecular Engineering and Department of Chemistry and Biochemistry, University of Maryland, College Park, Maryland 20742, United States

Supporting Information

ABSTRACT: Nanometallic fuels with high combustion enthalpy, such as aluminum, have been proposed as a potential fuel replacement for conventional metallic fuel to improve propellant performance in a variety of propulsive systems. Nevertheless, nanometallic fuels suffer from the processing challenges in polymer formulations such as increased viscosity and large agglomeration, which hinder their implementation. In this letter, we employ electrospray as a means to create a gel within a droplet, via a rapid, solvent evaporation-induced aggregation of aluminum nanoparticles, containing a small mass fraction of an energetic binder. The gelled aluminum microspheres were characterized and tested for their burning behavior by rapid wire heating ignition experiments. The gelled aluminum microspheres show enhanced combustion behavior compared to nanoaluminum, which possibly benefits from the nitrocellulose coating and the gelled microstructure, and is far superior to the corresponding dense micrometer-sized aluminum.

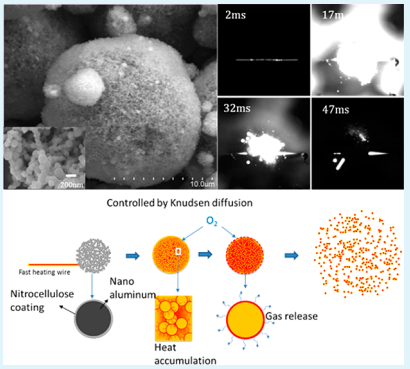

KEYWORDS: *electrospray, sol−gel, nanoaluminum, microspheres, nitrocellulose, combustion*

Because of its high enthalpy and ready availability, conventional aluminum powders with an average size of 3−20 μm are commonly employed in solid rocket propellant and other propulsive systems.[1−3] Although the energy density is increased after incorporation of micrometer-sized aluminum fuel in propellant systems, the burning rate however was not found to improve much, resulting in low rates of energy release.[4] Additionally, the oxide coating on the surface of microsized aluminum sufficiently passivates the fuel to a high ignition temperature ~2300 K.[2,5,6] In contrast, the use of nanoscale aluminum lowers the ignition temperature to <1000 K, with a much enhanced burning rate, and a lower ignition delay time.[6−12] Unfortunately nanometallic fuels suffer from processing challenges, that have significantly retarded their utility, most primarily because their very high surface area/small particle size increases the viscosity of polymer binder and oxidizer mix, such that high mass fractions of fuel cannot be formulated.[9,13−16]

One approach to deal with this issue is to directly incorporate the nanosized metallic fuel in energetic nanofibers.[17] This is not an ideal situation either, since the fibers themselves must be processed. There are other approaches, such as arrested milling to produce micrometer Al with nano features.[18−23]One alternative approach we will describe here is to maintain the nanostructure characteristics that make nanoaluminum desirable, but formulate them into a structure that is microsized.[24,25] Even though its density and energy density should be lower than micrometer Al, this micrometer-structured particle has the advantage that it can be processed using traditional methods for micrometer aluminum, while still maintaining its nano characteristics. It is also possible that the pores can be filled with other polymeric materials or additives, a topic we are currently exploring.

Electrospray approaches have been demonstrated as a simple method for the fabrication of nano/micro spheres, and is based on liquid jet break-up under the influence of a strong electric force.[26−29] Compared with other wet chemistry methods, electrospray provides a facile one-step approach to generate relatively uniform microspheres.[30] Other spraying methods can also assemble nanoparticles into microspheres.[31−33] But uniquely, the electrospray method has the advantage of producing nano/micro particles with a narrow size distribution. Additionally, precursor suspensions with high mass loading of particles and polymer solution are more easily sprayed by this electrostatic assist, making this approach particularly useful to produce polymer-based composite materials. Furthermore, the possible control and tuning of microparticle composition, size and morphology by electrospray exceeds that of conventional spray methods.[34−38]

In this letter, we employ electrospray as a means to create a gel within a droplet by evaporation induced rapid aggregation of aluminum nanoparticles, containing a small mass fraction of an energetic binder. In particular, nitrocellulose is introduced into the precursor solution and serves both as the energetic polymer binder but also to tune the final particle size and morphology. The gelled aluminum microparticles show

Received: April 8, 2013
Accepted: June 24, 2013
Published: July 22, 2013

   dx.doi.org/10.1021/am401238t | *ACS Appl. Mater. Interfaces* 2013, 5, 6797−6801

enhanced burning behavior compared to nanoaluminum (n-Al), which possibly benefits from the nitrocellulose coating and the gelled structure.

The electrospray formation of composite microparticles is conceptually simple, as illustrated in Figure 1. Aluminum

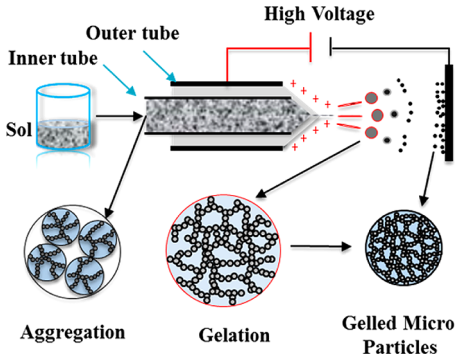

Figure 1. Schematic of electrospray formation of gelled nano-Al microspheres.

nanoparticles (ALEX, <50 nm, Argonide Corp., see Figure S1 in the Supporting Information) are dispersed into a nitrocellulose polymer solution and electrosprayed to form microdroplets, which are further dried to form microparticles after solvent removal. In a typical experiment, aluminum nanoparticles were dispersed into a colloidon solution (~17 mg/mL), and then sonicated and stirred to form a suspension. The suspension was then injected by coaxial capillary tubes (see Figure S2 in the Supporting Information), the inner diameter of inner tube (22 gauge steel) and the outer tube (17 gauge steel) is 0.41 and 1.07 mm, respectively, fed by two syringe pumps and electrosprayed to form gelled aluminum microparticles. Details of the experimental process could be found in the Supporting Information. Any operations were carefully processed with using gloves in case of electric shock, and the electrospraying process should be kept in a hood fume to release the organic solvent vapor.

Figure 2 shows scanning electron microscopy (SEM) image of electrosprayed gelled samples. The particles are found to be

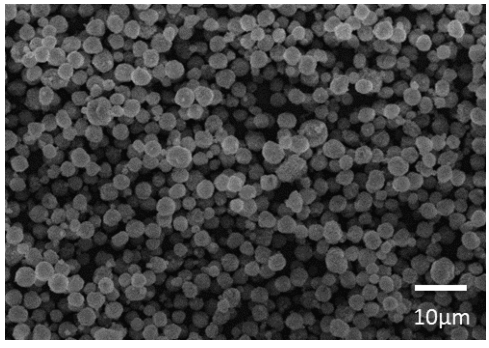

Figure 2. SEM image of aluminum microspheres produced by electrospraying. (Inner tube flow rate: 0.5 mL/h).

highly spherical with diameters of several micrometers, which can be varied depending on the Al nanoparticle concentration, and nitrocellulose content.

Unlike the sample of Figure 2, which employed both the inner and outer coaxial needle, the sample of Figure 3 only used inner tube. A close up view in Figure 3a reveals a porous

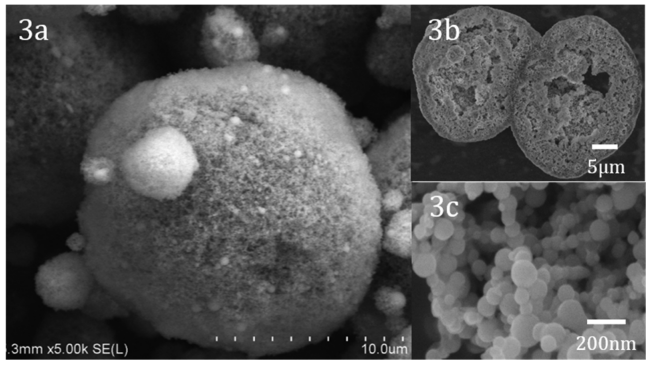

Figure 3. SEM images of (a) a typical gelled microsphere, (b) cross section, (c) high magnification SEM image of gelled microsphere.

structure of gelled aluminum microparticles with a diameter of ~16 μm (10 wt % NC). The flow rate in this single needle process was 4.5 mL/h. According to the relationship between droplet size and flow rate,[26,36] the average size of these microspheres should be larger than those produced by the coaxial needle electrospray process shown in Figure 2, which is consistent with our results. Also seen in Figure 3a are some smaller particles, which can be ascribed to fission of the primary droplets by Coulombic crowding.[39] Cross-section SEM images in Figure 3b and a high-resolution SEM image in Figure 3c further reveals the porous structure of the microparticle, which shows that while some cavities exist within the microparticles, for the most part the gel extends throughout the particle. It appears, however, that the surface region is denser than the interior, presumably because of aggregates on the surface having more opportunity to move and rearrange relative to the interior aggregates. The surface topology at still higher magnification (Figure 3c) shows that the structure has retained the primary particle structure comprising the gel. Brunauer–Emmett–Teller (BET) measurements indicate a surface area of 20 m^2 g^{-1} for the gelled aluminum microparticles shown in Figure 3a–c, which is close to that for an individual ~50 nm aluminum nanoparticle, implying that the whole microparticle structure is accessible. Thus on a per unit mass basis the specific surface area of the gelled microparticle is equivalent to the individual primary particles. This latter point is important for the expectation of high or comparable reactivity to the nascent aluminum nanoparticles. On the other hand one should expect that it is the exposed outer surface of the mesosphere that will have the most impact on the viscous behavior in a formulation. As shown in Figure 1, the chains of NC with nano-Al aggregate in the prepared semidiluted sol. With the evaporation of solvent within the droplets, the aggregate chains experience crowding and jam against each other to progressively create a three-dimensional porous network, which serves as the main structural skeleton, that is stabilized by the nitrocellulose polymer binder to create the gelled microparticles.[40,41] The SEM image and elemental mapping clearly demonstrate that the gelled aluminum microparticle has a homogeneous structure with uniform interdispersion of nano-Al and nitrocellulose polymer binder (Figure.S4).

We find that the average size of the gelled microparticles can be systematically changed from 2 to 16 μm by increasing the nano-Al particle concentration in the precursor solution, as shown in Figure 4. The fact that the particle size increases so dramatically by changing particle loading implies that larger droplets are being generated by the electrospray, presumably

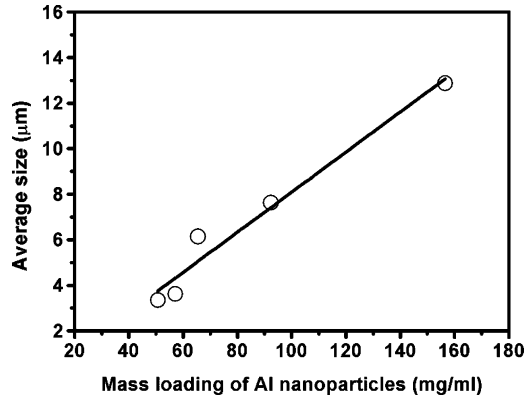

Figure 4. Average gelled particle size can be systematically increased by adding more nano-Al.

because the increased precursor solution viscosity rises with increased particle loading.[42,43] We found we could create even larger microspheres (~40 μm) by further increasing the flow rate.

The reactivity of these gelled microparticles was evaluated by coating a thin platinum wire (diameter 76 μm), which could be rapidly heated to measure the ignition delay time and temperature.[44] The wire was ramped to ~1600 K in 3 ms, at a heating rate of $\sim 4 \times 10^5$ K s^{-1}.[45] The burning process was recorded by a high-speed camera at the speed of 67000 frames per second to determine the time of sample ignition relative to the heating pulse, and temperature of the wire. For comparison purposes, nano-Al particles, nano-Al mixed with nitrocellulose, as well as microsized aluminum were also tested.

We propose the following conceptual mechanism of this enhanced burning as illustrated in Figure 6. With nitrocellulose's low decomposition temperature (170 °C), we expect gas generation to occur early during the heating process and combustion to commence with the oxygen within the porous structure. Unlike isolated nanoparticles undergoing oxidation that have high heat loss to the surrounding, rapid reaction within the gelled microparticle should be self-accelerating, because the heat of reaction is trapped within the microparticle, resulting in cooperative heating. Eventually, it is also possible that this rapid accumulation of heat and increasing rapid reaction lead to sufficient gas generation so as to overpressure

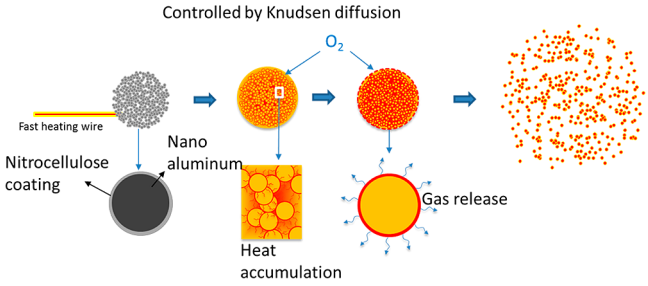

Figure 6. Proposed combustion process of gelled Al microparticles.

the structural integrity of the gel and shatter it into isolated burning nanoparticles, as evidenced by the large fire ball seen in Figure 5a.

The results of rapid wire heating experiments are presented in Table 1. Solid micrometer aluminum which has approximately the same size distribution as gelled microspheres, could not be ignited by our fast-heating wire because of the much higher ignition temperature (~2300 K) needed exceed the capabilities of our wire (1600 K).

Table 1. Ignition Delay and Burn Time Averaged over Three Experiments for Different Formulations[a]

material	ignition delay time (ms)	burn time (ms)
micrometer-sized Al (3.0–4.5 μm)	no ignition	0
nano Al powder (50 nm)	14.1	14
mixture of nano Al and NC (10%)	7.2	14
gelled particles (NC, 1% by mass)	13.2	18
gelled particles (NC, 3 wt %, mean size: 2.0 μm)	3.5	46
gelled particles (NC, 6.5 wt %, mean size: 3.1 μm)	1.1	56
gelled particles (NC, 10 wt %, mean size: 11.1 μm)	0.3	64

[a]The fast-heating snapshots of micrometer size Al, the mixture of nano Al and NC (10%, by mass) can be found in the Supporting Information (Figure S5a, b, respectively).

We noticed that for gelled particles, the ignition delay time is largely reduced from 14 ms to ~3.5 ms by adding 3 wt % NC. With the further increase of NC, the gelled microspheres show

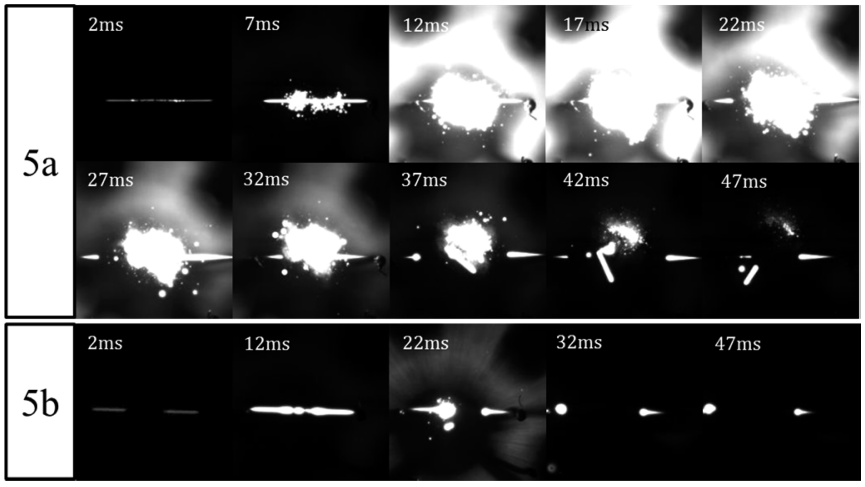

Figure 5. High speed video images: (a): Gelled aluminum microparticles; (b) Nanoaluminum. The labeled numbers are time elapsed after triggering.

dx.doi.org/10.1021/am401238t | ACS Appl. Mater. Interfaces 2013, 5, 6797–6801

shorter ignition delay, decreasing to 0.3 ms (10 wt %) while the burning duration increasing from 46 ms (3 wt %) to 64 ms (10 wt %). It has been found that the burning time of Al/NC composites is 2−5 times longer than Al nanoparticles. However, the burning time of the nano Al and NC (10 wt %) mixture remains the same as the pure Al nanoparticles.

As seen in Figure 5 and Table 1, the gelled aluminum microparticle (10 wt % NC) showed by far the highest burning duration of ∼64 ms and the shortest ignition delay time of ∼0.26 ms, indicating its better combustion performance than nano-Al powder (or nano-Al/NC mixture). The addition of NC serves as both a binder and as an energetic source, which could decrease the ignition delay due to its low decomposition temperature. We attribute the fast reactivity of the gelled material to the localization of the heat release. It is well-known, that nanoparticles are pyrophoric, but only when in sufficient high concentration. An isolated nanoparticle in air will not burn because of rapid heat loss to the surroundings.[46] The gelled particle is in effect an extreme example of this phenomena. The porous nature of the gel enables rapid oxygen transport while the constrained nature of the microspheres constrains the heat released within a small volume, which promotes acceleration of the global reaction. With 1 wt % NC, the nano-Al agglomerates together instead of forming gelled microspheres (see Figure S6 in the Supporting Information), which consequently has the similar burning behavior as the nano-Al. Increasing NC content results in an increase in particle size. As seen in Table 1 the particles with increased NC have a shorted ignition delay time, but because increasing NC also leads to larger particles, we observe an increased burning time.

In summary, gelled aluminum microspheres with a narrow size distribution were synthesized by a one-step electrospray method. The microstructures of the composite particles reveal a porous gelled inner structure with nano features. We show that the average microparticle size can be tuned over a relatively large range. Most interesting, however, is that these gelled aluminum microspheres show superior reactivity, than the nascent nanoparticle comprising the gelled particle. We expect that the unique gelled microparticle structure with nano building blocks could potentially circumvent the problems associated with trying to utilize nanometals in propellants.

■ ASSOCIATED CONTENT

Ⓢ Supporting Information

Detailed experimental procedures, SEM image and elemental mapping of gelled aluminum microspheres, rapid wire ignition of aluminum samples. This material is available free of charge via the Internet at http://pubs.acs.org.

■ AUTHOR INFORMATION

Corresponding Author

*E-mail: mrz@umd.edu. Phone: 301-405-4311. Fax: 301-314-947.

Present Address

[†]H.W., S.Y., and C.H. are currently at Nanjing University of Science and Technology, Nanjing, China

Notes

The authors declare no competing financial interest.

■ ACKNOWLEDGMENTS

This work was supported by the Defense Threat Reduction Agency and the Army Research Office. We acknowledge the support of the Maryland Nanocenter and its NispLab. The NispLab is supported in part by the NSF as a MRSEC Shared Experimental Facility. H.W. is grateful for the financial support from China Scholarship Council.

■ REFERENCES

(1) Arkhipov, V. A.; Korotkikh, A. G. *Combust. Flame* **2012**, *159*, 409−415.

(2) Sadeghipour, S.; Ghaderian, J.; Wahid, M. A. Advances in Aluminum Powder Usage As an Energetic Material and Applications for Rocket Propellant. In *4th International Meeting of Advances in Thermofluids*; Melaka, Malaysia, Oct 3−4, 2011 ; American Institute of Physics: Melville, NY, 2012; Vol. *1440*, pp 100−108.

(3) Dokhan, A.; Price, E.; Seitzman, J.; Sigman, R. *P. Proc. Combust. Inst.* **2002**, *29*, 2939−2946.

(4) Escot, B. P.; Chauveau, C.; Gökalp, I. *Aerosp. Sci. Technol.* **2007**, *11*, 33−38.

(5) Dreizin, E. L. *Prog. Energy Combust. Sci.* **2009**, *35*, 141−167.

(6) Yetter, R. A.; Risha, G. A.; Son, S. F. *Proc. Combust. Inst.* **2009**, *32*, 1819−1838.

(7) Jian, G. Q.; Chowdhury, S.; Sullivan, K.; Zachariah, M. R. *Combust. Flame* **2013**, *160*, 432−437.

(8) Muthiah, R.; Krishnamurthy, V.; Gupta, B. *J. Appl. Polym. Sci.* **1992**, *44*, 2043−2052.

(9) Meda, L.; Marra, G.; Galfetti, L.; Severini, F.; De Luca, L. *Mater. Sci. Eng., C* **2007**, *27*, 1393−1396.

(10) Puszynski, J. A.; Bulian, C. J.; Swiatkiewicz, J. J. *J. Propul. Powder* **2007**, *23*, 698−706.

(11) Sullivan, K.; Young, G.; Zachariah, M. *Combust. Flame* **2009**, *156*, 302−309.

(12) Armstrong, R. W.; Baschung, B.; Booth, D. W.; Samirant, M. *Nano Lett.* **2003**, *3*, 253−255.

(13) Zhi, J.; Shu-Fen, L.; Feng-Qi, Z.; Zi-Ru, L.; Cui-Mei, Y.; Yang, L.; Shang-Wen, L. *Propellants Explos. Pyrotech.* **2006**, *31*, 139−147.

(14) Lebedeva, E. A.; Tutubalina, I. L.; Val'tsifer, V. A.; Strel'nikov, V. N.; Astaf'eva, S. A.; Beketov, I. V. *Combust. Explos. Shock Waves* **2012**, *48*, 694−698.

(15) Wen, D. *Energy Environ. Sci.* **2010**, *3*, 591−600.

(16) Galfetti, L.; DeLuca, L.; Severini, F.; Colombo, G.; Meda, L.; Marra, G. *Aerosp. Sci. Technol.* **2007**, *11*, 26−32.

(17) Yan, S.; Jian, G.; Zachariah, M. R. *ACS Appl. Mater. Interfaces* **2012**, *4*, 6432−6435.

(18) Zhang, S.; Badiola, C.; Schoenitz, M.; Dreizin, E. L. *Combust. Flame* **2012**, *159*, 1980−1986.

(19) Sippel, T. R.; Son, S. F.; Groven, L. J. *Propellants Explos. Pyrotech.* **2013**, *38*, 286−295.

(20) Schoenitz, M.; Ward, T. S.; Dreizin, E. L. *Proc. Combust. Inst.* **2005**, *30*, 2071−2078.

(21) Schoenitz, M.; Ward, T. S.; Dreizin, E. L. *Mater. Res. Soc. Proc.* **2003**, *800*, 1−6.

(22) Dreizin, E. L. *Prog. Energy Combust. Sci.* **2009**, *35*, 141−167.

(23) Sippel, T. R.; Son, S. F.; Groven, L. J. *Propellants Explos. Pyrotech.* **2013**, *38*, 286−295.

(24) Polshettiwar, V.; Baruwati, B.; Varma, R. S. *ACS Nano* **2009**, *3*, 728−736.

(25) Yu, D. G.; Yang, J. H.; Wang, X.; Tian, F. *Nanotechnology* **2012**, *23*, 105606.

(26) Loscertales, I. G.; Barrero, A.; Guerrero, I.; Cortijo, R.; Marquez, M.; Ganan-Calvo, A. M. *Science* **2002**, *295*, 1695−1698.

(27) Jaworek, A. *Powder. Technol.* **2007**, *176*, 18−35.

(28) Jaworek, A.; Sobczyk, A. T. *J. Electrostat.* **2008**, *66*, 197−219.

(29) Bock, N.; Woodruff, M. A.; Hutmacher, D. W.; Dargaville, T. R. *Polymers* **2011**, *3*, 131−149.

(30) Chakraborty, S.; Liao, I. C.; Adler, A.; Leong, K. W. *Adv. Drug Delivery Rev.* **2009**, *61*, 1043−1054.

(31) Takashima, Y.; Saito, R.; Nakajima, A.; Oda, M.; Kimura, A.; Kanazawa, T.; Okada, H. *Int. J. Pharm.* **2007**, *343*, 262−269.

(32) Peltonen, L.; Valo, H.; Kolakovic, R.; Laaksonen, T.; Hirvonen, J. *Expert Opin. Drug Delivery* **2010**, *7*, 705−719.
(33) Yu, Z.; Garcia, A. S.; Johnston, K. P.; Williams, R. O. *Eur. J. Pharm. Biopharm.* **2004**, *58*, 529−537.
(34) Hogan, C. J.; Yun, K. M.; Chen, D.-R.; Lenggoro, I. W.; Biswas, P.; Okuyama, K. *Colloids Surf., A.* **2007**, *311*, 67−76.
(35) Almeria, B.; Deng, W.; Fahmy, T. M.; Gomez, A. *J. Colloid Interface Sci.* **2010**, *343*, 125−133.
(36) Ganan-Calvo, A. M.; Davila, J.; Barrero, A. *J. Aerosol Sci.* **1997**, *28*, 249−275.
(37) Loscertales, I. G.; Barrero, A.; Guerrero, I.; Cortijo, R.; Marquez, M.; Ganan-Calvo, A. M. *Science* **2002**, *295*, 1695−1698.
(38) Gañán-Calvo, A. M. *Phys. Rev. Lett.* **1997**, *79*, 217−220.
(39) Bock, N.; Dargaville, T. R.; Woodruff, M. A. *Prog. Polym. Sci.* **2012**, *37*, 1510−1551.
(40) Abete, T.; Del Gado, E.; de Arcangelis, L. *Polym. Compos.* **2013**, *34*, 259−264.
(41) Gromov, A.; Ilyin, A.; Förter-Barth, U.; Teipel, U. *Propellants Explos. Pyrotech.* **2006**, *31*, 401−409.
(42) Omland, T. H.; Dahl, B.; Saasen, A.; Svanes, K.; Amundsen, P. A. *Annu. Trans. Nordic Rheol. Soc.* **2005**, *13*, 107−110.
(43) Bicerano, J.; Douglas, J. F.; Brune, D. A. *Rev. Macromol. Chem. Phys.* **1999**, *C39*, 561−642.
(44) Wu, C.; Sullivan, K.; Chowdhury, S.; Jian, G.; Zhou, L.; Zachariah, M. R. *Adv. Funct. Mater.* **2012**, *22*, 78−85.
(45) Jian, G.; Piekiel, N. W.; Zachariah, M. R. *J. Phys. Chem. C* **2012**, *116*, 26881−26887.
(46) Krause, U.; Schmidt, M.; Lohrer, C. A. *J. Loss Prev. Process Ind.* **2006**, *19*, 218−226.